Percolation and cluster structure parameters: The radius of gyration

1997 J. Phys. A: Math. Gen. 30 8459

(http://iopscience.iop.org/0305-4470/30/24/011)

J. Phys. A: Math. Gen. **30** (1997) 8459–8469. Printed in the UK PII: S0305-4470(97)83414-2

Percolation and cluster structure parameters: The radius of gyration

Joseph Hoshen†
812 Shiloh Circle, Naperville, IL 60540-7112, USA

Received 14 April 1997, in final form 27 June 1997

Abstract. The squared radius of gyration of percolation clusters are determined in terms of the clusters' second spatial moments using the enhanced Hoshen–Kopelman algorithm for square and triangular lattices containing 2.025×10^9 sites. Correlation length exponents and related exponents as well as their corresponding amplitudes are calculated in terms of the squared radius of gyration above and below the percolation threshold. A coefficient for cluster compactness that is based on the squared radius of gyration of a cluster is introduced. That coefficient is compared with a similar coefficient of compactness that is based on the cluster cyclomatic number.

1. Introduction

Since the introduction of percolation theory, the focus of cluster analysis in Monte Carlo simulation has been on quantities that can be derived from cluster sizes [1]. Cluster structure or shape information has received somewhat less attention, possibly, because the computational tools for calculating structure parameters are not as powerful as those that are used for determining cluster sizes. Cluster structure calculations usually involve relatively small lattices when compared with cluster size calculations which very often employ lattices containing 10^9 sites or more. For example, Rapaport [2] reported cluster size calculations for a lattice containing 4.225×10^{11} sites.

A very important cluster structure parameter is the squared radius of gyration, which is a measure for the mean distance between two sites belonging to the same cluster. Stauffer and Aharony [1] suggested a relationship between the radius of gyration and the fractal dimension of the lattice. They also suggested relationships between the radius of gyration and the correlation length and other related squared distance parameters. Other researchers have provided us with examples of computed cluster structure parameters, which include perimeters [3], correlation length [4], backbone perimeter [5], and spanning lengths [6]. A more recent study focuses on exponents for the end-to-end distance distribution between two cluster sites at criticality [7].

Quandt and Young [8] calculated the gyration tensor to determine the cluster asphericity parameters of Rudnic and Gaspari [9] for percolation and Ising clusters. They applied the Hoshen–Kopelman (HK) [10] algorithm to identify clusters. Yet, in their calculations, they only studied relatively small percolation clusters of sizes 5–4096.

Domb and Stoll [11] introduced the cyclomatic number as a structure parameter. They used the cyclomatic number, which represents the number of independent cycles in a cluster, to define a coefficient of cluster compactness.

† E-mail address: jhoshen@worldnet.att.net

0305-4470/97/248459+11$19.50

Recently, Hoshen *et al* [12] introduced the enhanced HK (EHK) algorithm for the structural analysis of clusters in binary lattices. The EHK algorithm was further enhanced for multiple colour image processing [13]. This enhanced algorithm can be used to calculate various cluster structure parameters in large lattices with the computational efficiency of the original HK algorithm [10]. The original HK algorithm makes a single pass through the lattice inspecting each site sequentially and assigning it with a cluster label. Each cluster in the lattice is identified by one or more labels. The EHK algorithm generalizes the HK method of cluster size calculation to the calculation of structural parameters such as spatial moments, cluster bounding rectangles and perimeters of all clusters in the lattice in a single pass [12]. To enable the EHK analysis of very large lattices while storing only a small fraction of the lattices in the computer's memory, we have used the label recycling method, denoted as option (c) in [10].

Using the EHK algorithm, in section 2, we provide results for the squared radius of gyration calculations for lattices containing 2.025×10^9 sites where the squared radius of gyration is determined from the clusters' spatial moments. We use the squared radius of gyration to calculate the correlation length and other parameters as suggested by Stauffer and Aharony [1]. In section 3, we introduce a cluster compactness coefficient, which is based on the squared radius of gyration, and compare it with the cyclomatic number coefficient of Domb and Stoll [11]. In section 4, we discuss our computation results.

2. The squared radius of gyration

A general expression for cluster spatial moments, M_k, in d dimensions is

$$M_k(m(1), m(2), \ldots, m(d)) = \sum_{i \in k} \prod_{\mu=1}^{d} x_\mu^{m(\mu)}(i) \tag{1}$$

where $x_\mu(i)$ denotes the μth coordinate of the ith site of the kth cluster and $m(\mu)$ is the exponent for the x_μ coordinate. When all $m(\mu) = 0$, (1) represents the zero moment of the cluster. This moment denotes the cluster size. The first cluster moment, which defines the cluster's centre of mass, for the μth coordinate is

$$M_k(m(1) = 0, m(2) = 0, \ldots, m(\mu) = 1, \ldots, m(d) = 0). \tag{2}$$

In a similar fashion, the second spatial cluster moment can be defined. In two dimensions, this would correspond to x^2, y^2 and xy terms.

Using the cluster moments, we can calculate the squared radius of gyration, R_s^2, given by:

$$R_s^2 = \frac{1}{2s^2} \sum_{i,j} |\boldsymbol{r}_i - \boldsymbol{r}_j|^2 \tag{3}$$

where s is the size of the cluster, $\boldsymbol{r}_i$ and $\boldsymbol{r}_j$ are the positions of sites i and j belonging to the cluster. The double summation is carried over all i and j sites of the cluster. It can be shown that R_s^2 can be given in terms of the cluster first and second moments [12]:

$$R_s^2 = \frac{1}{s^2} \sum_{\mu=1}^{d} [s X_\mu^{(2)} - (X_\mu^{(1)})^2] \tag{4}$$

where $X_\mu^{(1)} = \sum_i x_\mu(i)$ is the first moment and $X_\mu^{(2)} = \sum_i x_\mu^2(i)$ is the second moment.

In the remainder of this section, we shall use the EHK algorithm calculation of the squared radius of gyration to test the various relationships for the radius of gyration given

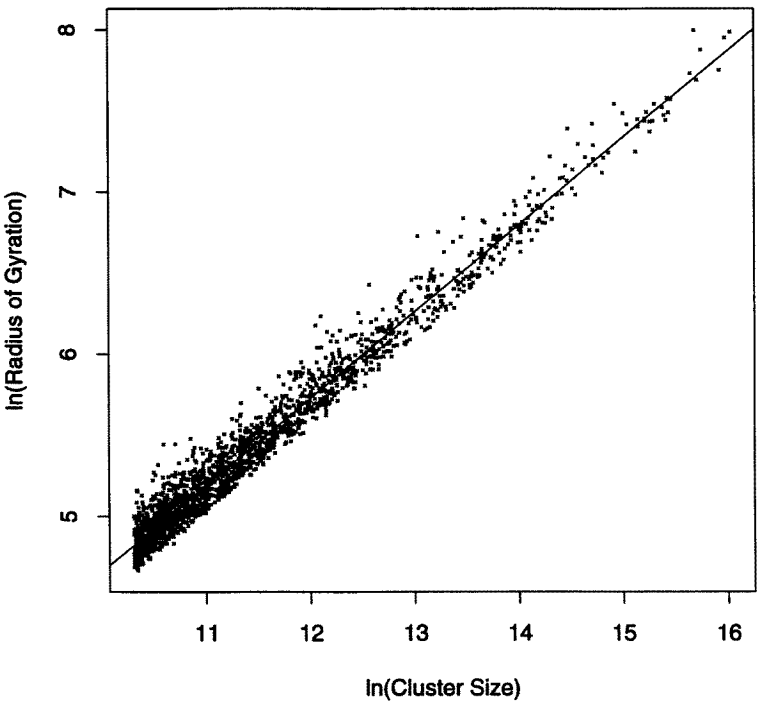

Figure 1. $\ln(R_s^2)$ versus $\ln(s)$ for $p = 0.592$ and for cluster sizes $100\,000 > s > 30\,000$ for $45\,000 \times 45\,000$ lattice.

Table 1. D^* values for some p values for a square lattice.

p	Number of clusters	D^*
0.580	1001	0.887 ± 0.022
0.585	4064	1.230 ± 0.005
0.590	4125	1.715 ± 0.004
0.592	1975	1.782 ± 0.005

by Stauffer and Aharony [1]. They suggest that at the percolation threshold, the following relationship exists between R_s^2 and s

$$R_s^2 \propto s^{1/D} \tag{5}$$

where D is the fractal dimension.

To test relationship (5), using the EHK algorithm, we computed R_s^2 values for clusters on a $45\,000 \times 45\,000$ simulated square lattice. Figure 1 displays the result of this computation for $p = 0.592$ and for cluster sizes $100\,000 > s > 30\,000$. The values of the exponent D^*, which were determined from the slope $T(D^* = T^{-1})$ of the line corresponding to a logarithmic transformation of (5), are given in table 1 for $p = 0.58, 0.585, 0.59, 0.592$. (We denote the exponents as D^* to distinguish them from D, which is defined for p_c.) Clearly, the D^* values increase as the percolation threshold is approached. At $p = 0.592$ the mean value of D^* is 1.782 indicating a slow convergence to the D_{exact} value of $\frac{91}{48} \approx 1.896$ [1].

D^* and other parameters reported in this paper were calculated using linear regression analysis. The error bars of these parameters were derived from the standard deviations in the linear regression coefficients [14]. For example, the error bar ΔD^* for the exponent D^* is $T^{-2}\Delta T$ where ΔT is the error bar for the gradient T of the regression line.

A Windows 95 166 MHz Pentium® PC was used for all EHK algorithm computations. The algorithm was implemented in *C*. The computation time for each Monte Carlo run on a $45\,000 \times 45\,000$ lattice took approximately 60 min and consumed about 3 MB of RAM. In all simulations free boundary conditions were used. In the simulations, we used a pseudorandom number generator suggested by Knuth [15]. That generator has a pseudorandom number sequence cycle that is at least $2^{55} - 1$ long.

Stauffer and Aharony [1] suggested three different definitions of a lattice averaged squared radius given in terms of R_s^2. These include the correlation length, ξ^2, and two other radii, which we denote as ξ_2^2 and ξ_3^2, where

$$\xi^2 = \frac{2\sum_s \langle R_s^2 \rangle s^2 n_s}{\sum_s s^2 n_s} \tag{6a}$$

$$\xi_2^2 = \frac{2\sum_s \langle R_s^2 \rangle s n_s}{\sum_s s n_s} \tag{6b}$$

$$\xi_3^2 = \frac{2\sum_s \langle R_s^2 \rangle n_s}{\sum_s n_s}. \tag{6c}$$

Below p_c the summation is carried over all clusters. Above p_c, the contribution of the largest cluster is excluded from the summation. n_s denotes the number of clusters of size s. $\langle R_s^2 \rangle$ stands for the mean squared radius of gyration over all clusters of size s. Near p_c, the following relationships are expected to hold, $\xi = \xi_{1,W}|p - p_c|^{-\nu}$, $\xi_2 = \xi_{2,W}|p - p_c|^{-(\nu-\beta/2)}$ and $\xi_3 = \xi_{3,W}|p - p_c|^{-J}$. ν and β are the critical exponents for the correlation length and the infinite cluster probability, respectively. J stands for a proposed exponent for (6*c*). The subscript W for the amplitudes $\xi_{1,W}, \xi_{2,W}$ and $\xi_{3,W}$ is set to B if $p < p_c$ and is set to A if $p > p_c$.

To calculate the amplitudes and exponents for ξ, ξ_2 and ξ_3, 92 Monte Carlo runs were made on square and triangular lattices containing $45\,000 \times 45\,000$ sites below and above p_c. Table 2 provides a summary for these run sequences. To ensure that pseudorandom number sequences do not overlap within a run sequence, the last random number seed of a run was used to generate a new seed for the next run. Square boundaries were used for the square lattice simulations and rhombus boundaries were used for the triangular lattice simulation. In the calculation, we used $p_c = 0.5$ for the triangular lattice, and $p_c = 0.592\,746$ for the square lattice [1]. Figure 2 gives a log–log plot for ξ, ξ_2 and ξ_3 for the square lattice data below p_c. The amplitudes $\xi_{I,W}$ and their error bars are determined from the intercept V of the regression line, such that $\xi_{I,W} = \exp(V)$ and $\Delta\xi_{I,W} = \exp(V)\Delta V$ where $I = 1, 2, 3$ and ΔV is the statistical error for V [14].

Table 2. Simulation run sequences.

Lattice	Data points	p range
square	32	0.52–0.58
square	19	0.601–0.624
triangular	22	0.425–0.48
triangular	19	0.51–0.5325

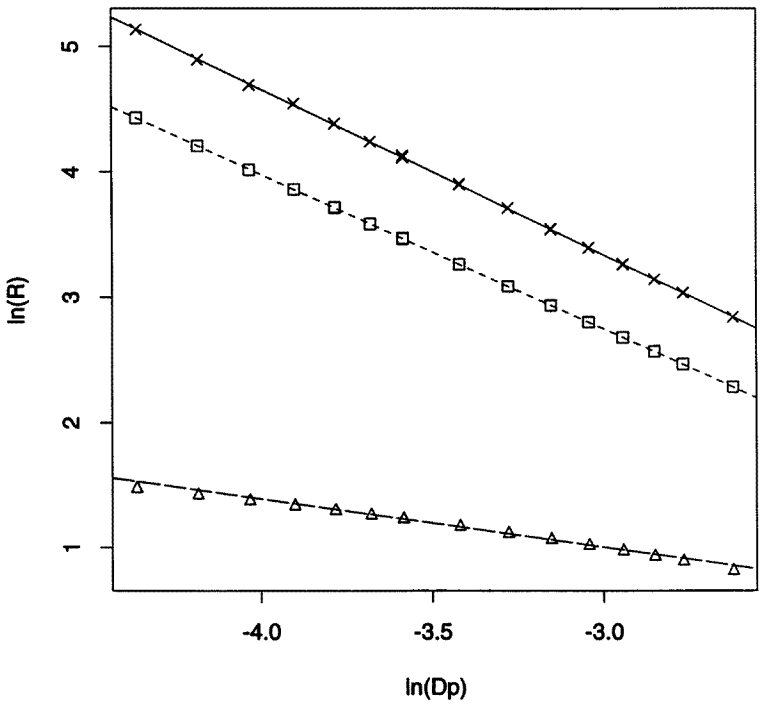

Figure 2. $\ln(R)$ versus $\ln(Dp)$ where $Dp = |p_c - p|$ for 32 runs, p =0.52–0.58 (some p values are repeated) and 45 000 × 45 000 lattice size. When $R = \xi$, corresponding to (6*a*), data points shown as × and —— denotes the regression line. When $R = \xi_1$, corresponding to (6*b*), data points are shown as □ and - - - - denotes the regression line. When $R = \xi_2$, corresponding to (6*c*), data points shown as Δ and – – – denotes the regression line.

Table 3. Lattice mean squared radii exponents and amplitudes for (6*a*)–(6*c*) for square and triangular lattices.

			Below p_c		Above p_c	
Lattice radius	Lattice type	Exponent	Computed exponent	$\xi_{I,B}$	Computed exponent	$\xi_{I,A}$
ξ	square	ν	1.320 ± 0.002	0.539 ± 0.004	1.39 ± 0.07	0.12 ± 0.03
ξ_2	square	$\nu - \beta/2$	1.233 ± 0.001	0.385 ± 0.001	1.05 ± 0.01	0.13 ± 0.01
ξ_3	square	J	0.390 ± 0.006	0.845 ± 0.019	0.33 ± 0.01	0.36 ± 0.01
ξ	triangular	ν	1.343 ± 0.002	0.460 ± 0.003	1.35 ± 0.05	0.12 ± 0.02
ξ_2	triangular	$\nu - \beta/2$	1.244 ± 0.001	0.348 ± 0.001	1.02 ± 0.01	0.14 ± 0.01
ξ_3	triangular	J	0.359 ± 0.010	1.085 ± 0.034	0.32 ± 0.01	0.44 ± 0.01

The results for the exponents, their amplitudes and error bars for square and triangular lattices above and below p_c are summarized in table 3. We should note that the statistical error bars for both the square and triangular lattices were larger above p_c than below it. The computed ν exponent values for both the square and triangular lattices below and above p_c are scattered around 1.35 which is close to $\nu_{\text{exact}} = \frac{4}{3} \approx 1.333$ [1]. In table 3 we observe that below p_c $\nu - \beta/2 \approx 1.23$ for the square and triangular lattices, and that above p_c

Table 4. Results for p_c and amplitudes, $\xi_{1,W}$, for (7) and (8) for square and triangular lattices.

Lattice	Data points range	p_c [a]	$\xi_{1,W}$ [a]	$\xi_{1,W}$ [b]
square	below p_c	0.5930 ± 0.0001	0.522 ± 0.001	0.516 ± 0.004
square	above p_c	0.594 ± 0.001	0.13 ± 0.01	0.14 ± 0.01
triangular	below p_c	0.4996 ± 0.0001	0.471 ± 0.001	0.475 ± 0.004
triangular	above p_c	0.501 ± 0.001	0.14 ± 0.01	0.15 ± 0.01

[a] Value determined using (7).
[b] Value determined using (8).

$\nu - \beta/2 \approx 1.03$. Yet for both lattices, these values differ by 0.2.

It is worth noting that below p_c, $\nu_{\text{exact}} - \beta_{\text{exact}}/2 = \frac{91}{72} \approx 1.264$ is close to the calculated values of 1.233 and 1.244 for the square and triangular lattices given in table 3. Furthermore, $D = d - \beta/\nu = d - 2 + 2(\nu - \beta/2)/\nu$. Since $d = 2$, $D = 2(\nu - \beta/2)/\nu$. Using the below p_c values of ν and $(\nu - \beta/2)$ from table 2, we obtain $D = 1.868$ for the square lattice and $D = 1.853$ for the triangular lattice which compares rather well with $D_{\text{exact}} = \frac{91}{48} \approx 1.896$.

For the proposed exponent J, we note that for both square and triangular lattices below and above p_c, $J \approx 0.4$, which differs from the value of 0 suggested in [1].

Using our numerical results and setting ν to ν_{exact}, we can calculate p_c. We transform $\xi = \xi_{1,W}|p_c - p|^{-\nu}$ to

$$p = p_c + Q\xi^{-1/\nu} \tag{7}$$

where $Q = -\xi_{1,B}^{1/\nu}$ for $p_c > p$ and $Q = \xi_{1,A}^{1/\nu}$ for $p > p_c$. In (7), both p_c and Q are unknown, and we set ν to ν_{exact}. We can calculate p_c and Q from the intercept and gradient of p versus $\xi^{-1/\nu}$. The error bars for $\xi_{1,W}$ are $\nu|Q|^{\nu-1}\Delta Q$ where ΔQ is the statistical error for Q. Using linear regression analysis for (7) and assuming $\nu = \nu_{\text{exact}}$ and employing data points of table 2, we calculated p_c and $\xi_{1,w}$. Table 4 presents results for p_c and $\xi_{1,W}$ in columns 3 and 4, respectively.

If p_c is known in addition to ν_{exact}, we can calculate $\xi_{1,W}$ using the following expression:

$$\xi_{1,W} = \xi|p_c - p|^{\nu}. \tag{8}$$

Setting $\nu = \nu_{\text{exact}}$, and $p_c = 0.5$ for the triangular lattice and $p_c = 0.592\,746$ for the square lattice in (8), we calculate $\xi_{1,W}$. Results for this calculation are presented in column 5 of table 4.

The calculated values for the square lattice for the amplitudes, $\xi_{1,B}$, below p_c, are 0.539 (table 3), and 0.522 (table 4 column 4) and 0.516 (table 4 column 5); for the triangular lattice they are 0.460 (table 3), 0.471 (table 4 column 4) and 0.475 (table 4 column 5). They are close to the value of 0.52 calculated by Aharony and Stauffer [16] for both the square and triangular lattices, which is different from the value of 0.63 given by Corsten *et al* [17]. Furthermore, the amplitude ratios $\xi_{1,B}/\xi_{1,A}$ for both the square and triangular lattices is about 4 which is also consistent with [16, 17]. Chayes *et al* [18] gave a ratio of 2 instead of 4 by using a different definition of the correlation length.

3. Bounds on the radius of gyration

The squared radius of gyration, R_s^2, is a useful cluster structure quantity. It is a measure for the mean square distance between two cluster sites and, therefore, it is a measure for cluster compactness. Yet, just knowing that a given cluster has some R_s^2 value does not tell

us how compact or ramified the cluster in question is. In a similar fashion to Domb and Stoll [11], who proposed a coefficient of compactness, λ, based on the cyclomatic number, we could define cluster compactness relative to the upper and lower bounds of R_s^2.

The upper bound, $R_{s,\max}^2$, for R_s^2 occurs when the cluster is linear. Since R_s^2 is an invariant quantity under translation (and rotation), we can place a linear cluster of size s on the x-axis at $x = 1$. Using the summation formulae for $1 + 2+, \ldots, +s$ and $1^2 + 2^2+, \ldots, +s^2$, and (4), we obtain

$$R_{s,\max}^2 = \frac{s^2 - 1}{12}. \tag{9}$$

For large s, $R_{s,\max}^2$ can be written as

$$R_{s,\max}^2 = \frac{s^2}{12} \tag{9a}$$

where (9) and (9a) are true for linear clusters in any dimension.

To determine $R_{s,\min}^2$, the lower bound for R_s^2, in two dimensions, we assume that the most compact cluster of size s is bounded by a circle of radius r, whose area is equal to the area covered by the cluster. For a square lattice, given that the distance between nearest neighbours is 1, the density of sites is also 1. Therefore, we have $s = \pi r^2$. For a large s, we change the summation in (4) into integration and assume that the centre of mass for the cluster is at the origin. We obtain

$$R_{s,\min}^2 = \frac{1}{s}\int_0^{2\pi} \mathrm{d}\theta \int_0^r \rho^2 \rho \,\mathrm{d}\rho = \frac{\pi r^4}{2s} = \frac{s}{2\pi}. \tag{10}$$

We can also calculate a similar $R_{s,\min}^2$ for a simple cubic lattice for the compact cluster bounded by a sphere. We use now (4) for a sphere whose centre is at the origin. We replace summation by integration for $X_\mu^{(2)}$ and noting that the volume of the sphere is $s = 4\pi r^3/3$, we obtain

$$R_{s,\min}^2 = \frac{1}{s}\int_0^{\pi} \mathrm{d}\theta \int_0^{2\pi} \mathrm{d}\phi \int_0^r \rho^2 \sin\theta \rho^2 \,\mathrm{d}\rho = \frac{4\pi r^5}{5s} = \frac{3}{5}\left(\frac{3s}{4\pi}\right)^{2/3}. \tag{11}$$

We assumed again that the density of sites is 1. For other lattice types, the density of sites would be higher or lower than 1 depending on the density of sites in a unit square (or cube). However, the exponent of s would only depend on the dimension of the lattice.

Equations (10) and (11), apply to a large s only. For small clusters, we employ an algorithm to compute $R_{s,\min}^2$. This algorithm is based on a recursive representation of (4). To do that, we express R_s^2 in the coordinate system of the centre of the mass of the cluster, so that R_s^2 simplifies to

$$R_s^2 = \frac{1}{s}\sum_{\mu=1}^{d}\sum_i x_{\mu,i}^2 \tag{12}$$

$x_{\mu,i}$ is the μth coordinate of the ith site of the cluster. Using (4) and adding one more site to our cluster, we obtain

$$R_{s+1}^2 = \frac{1}{(s+1)^2}\sum_{\mu=1}^{d}[(s+1)X_\mu^{(2)} - (X_\mu^{(1)})^2]. \tag{13}$$

Writing (13) in terms of the centre of mass of the original cluster of size s, we get a recursive relationship for R_s^2:

$$R_{s+1}^2 = s\left[\frac{R_s^2}{s+1} + \frac{\sum_{\mu=1}^{d} x_{\mu,s+1}^2}{(s+1)^2}\right] \tag{14}$$

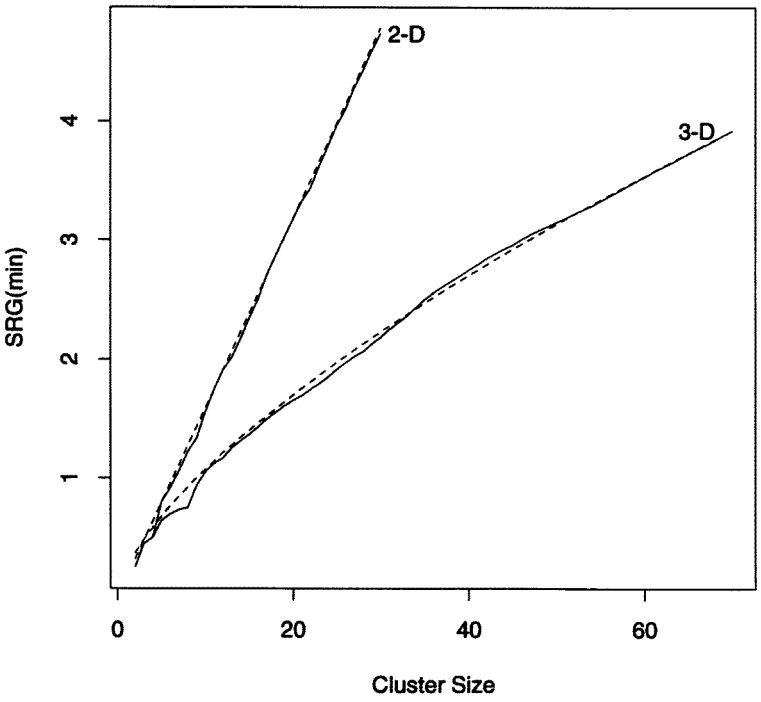

Figure 3. Squared radius of gyration for the compact cluster (SRG(min)), $R^2_{s,\min}$, versus cluster size s for a square lattice, denoted as two dimensional; and cubic lattice, denoted as three dimensional. Full curves denote algorithm (14) results. Broken curves denote approximate results given by (10) and (11) for square and cubic lattices, respectively.

where $x_{\mu,s+1}$ is the μth coordinate of the new cluster site $s+1$ given in the coordinate system of the centre of mass of the s-sized cluster.

We now use recursively (14) to determine $R^2_{s,\min}$. The algorithm starts from a single site at the origin. It then inspects all empty neighbouring sites around that site such that $\sum_{\mu=1}^{d} x^2_{\mu,2}$ is minimized. When it finds a site that minimizes (14), the algorithm adds it to the cluster. The search process is repeated around the cluster for an empty site that minimizes $\sum_{\mu=1}^{d} x^2_{\mu,3}$ etc. Every time $\sum_{\mu=1}^{d} x^2_{\mu,s+1}$ is minimized, we make sure that we minimize it in terms of the coordinates of the centre of the mass of the previous cluster.

The justification for the algorithm is that at every iteration, we minimize R^2_s. However, such a minimum may be only a local minimum and not a global one. So, at this point, we should consider the algorithm to be a heuristic algorithm. Yet, when we compare the algorithm results with the approximate formulae, (10) and (11), for $R^2_{s,\min}$, we obtain good matches for $s > 40$ as shown in figure 3.

To measure cluster compactness, we define e as a coefficient of compactness:

$$e = \frac{(R^2_s)^{-1} - (R^2_{s,\max})^{-1}}{(R^2_{s,\min})^{-1} - (R^2_{s,\max})^{-1}}. \tag{15}$$

The value of e ranges from 0, for the linear cluster, to 1, for the most compact cluster. For large s, our simulations suggest that for most clusters $(R^2_{s,\min})^{-1} > (R^2_s)^{-1} \gg (R^2_{s,\max})^{-1}$ so that $e \approx R^2_{s,\min}/R^2_s$. Figure 4 displays e for several p values for clusters grouped by size. We observe that as the cluster size increases for a given p, the ratio e decreases, indicating

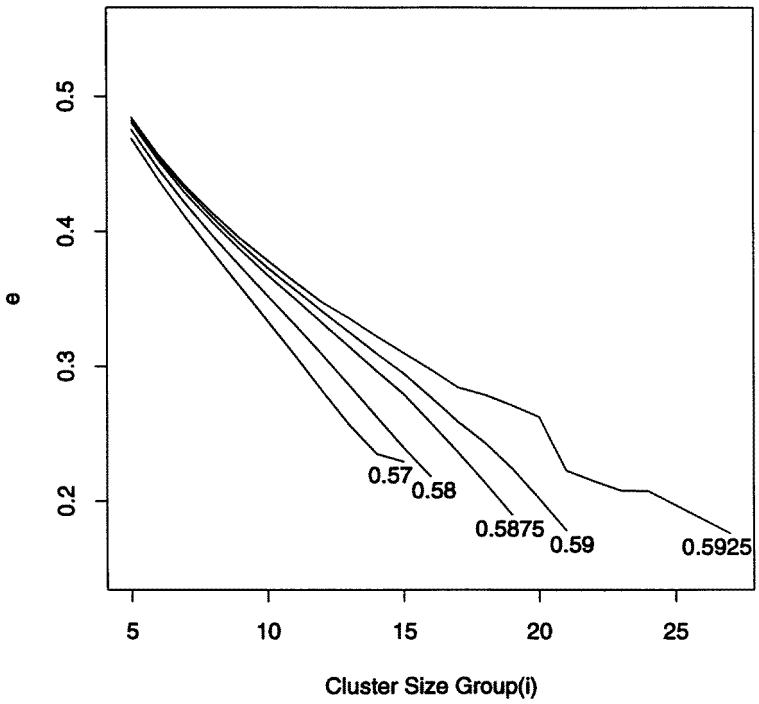

Figure 4. Cluster compactness coefficient, e, plotted versus cluster size groups i such that $2^i \leqslant s < 2^{i+1}$ for $p = 0.57, 0.58, 0.5875, 0.59, 0.5925$ for $45\,000 \times 45\,000$ lattices.

that the larger clusters are more ramified. On the other hand, clusters of a given size group become more compact as p increases.

At this point, it would be useful to compare the coefficient e with the coefficient λ given by Domb and Stoll [11]

$$\lambda = \frac{b - s + 1}{(s^{1/2} - 1)^2}. \tag{16}$$

In (16), b represents the number of bonds in the cluster. $b - s + 1$ is the cyclomatic number representing the number of independent cycles in the cluster and $(s^{1/2} - 1)$ represents the cyclomatic number for the most compact cluster of size s. The values of both e and λ range from 0 to 1. However, the value of 0 for λ does not distinguish between a linear cluster or a tree-like cluster. In contrast, $e = 0$ applies only to linear clusters. For tree-like clusters and other clusters, $e > 0$. When a cluster achieves maximum compactness, both λ and e are equal to 1. For large clusters, $\lambda = 1$ for both compact circular clusters and compact square clusters. $e = 1$ for only compact circular clusters. Using (15), (9*a*) and (10) for compact square clusters, we obtain $e = (3 - 3/s)/(\pi - 3/s) \approx 3/\pi$.

4. Discussion

With the help of the EHK algorithm, we approached the issue of cluster structure by studying the squared radius of gyration that is derived from the first and second spatial moments of the cluster. We used the squared radius of gyration to evaluate the correlation length and related parameters. We had a very good linear fit for the correlation length curve where

$\nu = 1.320 \pm 0.002$ for the square lattice and $\nu = 1.343 \pm 0.002$ for the triangular lattice below p_c. These values are close to the exact value of ν of $\frac{4}{3} \approx 1.333$. Since the statistical error bars are relatively small (0.002), systematic errors are the likely source for the differences between the calculated ν values and ν_{exact}. Examples of sources for systematic errors are pseudorandom number generators, the ranges of values of p used in the simulation, and the finite distance of p from the threshold. Nevertheless, because both calculated ν values for the square and triangular lattices were determined by the same method, the reasons for the 0.023 difference between these two values (11.5 error bars) requires further study.

The finite sizes and boundary shape of the lattices is likely to be another source of systematic errors. It appears that the boundary effects are more pronounced for large clusters cut off by the boundary. A simple example illustrates this point. At $p = 1$ in two dimensions, the squared correlation length for a square lattice with finite square boundaries is $\xi^2 = s/6$. On the other hand, according to (10), the squared correlation length for a square lattice bounded by a finite circle is $\xi^2 = s/(2\pi)$. The large clusters are significant contributors to the numerator of $(6a)$, and when they are cut, the value of the correlation length could be significantly affected. There are several approaches that could be used to address the problem. In one approach, we could remove the contributions of all clusters that touch the lattice boundary as was described in [16] for the Leath [19] algorithm calculations. Alternatively, we could use cyclic boundary conditions to extend the clusters across the boundary. Another approach would be to use only smaller p values so that there would be fewer large clusters stretching across the boundary.

The focus of this paper has been on low-order cluster spatial moments. Since the EHK algorithm can calculate higher moments for large lattices, the question is what new physical information can be derived from these higher-order moments. While raw moments are not very useful quantities by themselves, quantities that can be derived from them such as the squared radius of gyration are useful. For higher moments to become useful, there is a need to find quantities similar to the radius of gyration and express them in terms of these higher moments. These quantities should be defined with respect to the centre of mass of the cluster, thus, making them invariant to translation.

Acknowledgment

I would like to thank D Stauffer for his valuable help, comments and his suggestion for the study of the critical exponents amplitudes.

References

[1] Stauffer D and Aharony A 1994 *Introduction to Percolation Theory* 2nd edn (London: Taylor and Francis) pp 52–69
[2] Rapaport D C 1992 *J. Stat. Phys.* **66** 679
[3] Franke H 1980 *Z. Phys.* B **40** 61
[4] Kapitulnik A, Aharony A, Deutscher G and Stauffer D 1983 *J. Phys. A: Math. Gen.* **16** L269
[5] Manna S S 1989 *J. Phys. A: Math. Gen.* **22** 433
[6] Harrison R J, Bishop G H and Quinn G D 1978 *J. Stat. Phys.* **19** 53
[7] Roman H E 1995 *Phys. Rev.* E **51** 5422
[8] Quandt S and Young A P 1987 *J. Phys. A: Math. Gen.* **20** L851
[9] Rudnic J and Gaspari G 1986 *J. Phys. A: Math. Gen.* **19** L191
[10] Hoshen J and Kopelman R 1976 *Phys. Rev.* B **14** 3438
[11] Domb C and Stoll E 1977 *J. Phys. A: Math. Gen.* **10** 1141
[12] Hoshen J, Berry M W and Minser K S 1997 *Phys. Rev.* E **56** 1455
[13] Hoshen J unpublished

[14] Ben-Horin M and Levy H 1984 *Statistics, Decision and Applications in Business and Economics* 2nd edn (New York: McGraw-Hill) pp 588–9
[15] Knuth D E 1981 *The Art of Computer Programming Volume 2 Seminumerical Algorithms* (Reading, MA: Addison-Wesley) pp 171–2
[16] Aharony A and Stauffer D 1997 *J. Phys. A: Math. Gen.* **30** L301
[17] Corsten M, Jan N and Jerrard R 1989 *Physica* **156A** 781
[18] Chayes J T, Chayes L, Grimmett G R, Kesten H and Schonmann R H 1989 *Ann. Prob.* **17** 1277
[19] Leath P L 1976 *Phys. Rev.* B **14** 5046